EXPERIMENTAL AND COMPUTATIONAL INVESTIGATIONS OF ALFVÉN EIGENMODE STABILITY IN JET PLASMAS THROUGH ACTIVE ANTENNA EXCITATION

R.A. Tinguely, M. Porkolab, V. Aslanyan
Plasma Science and Fusion Center, Massachusetts Institute of Technology
Cambridge, Massachusetts, United States of America
Email: rating@mit.edu

N. Fil, S. Dowson, M. Fitzgerald, S.E. Sharapov
Culham Centre for Fusion Energy, Culham Science Centre
Abingdon, United Kingdom of Great Britain and Northern Ireland

P.G. Puglia, A. Fasoli, D. Testa
Ecole Polytechnique Fédérale de Lausanne, Swiss Plasma Center
Lausanne, Switzerland

D. Borba
Instituto de Plasmas e Fusão Nuclear, IST, Universidade de Lisboa
Lisbon, Portugal

R. Dumont
CEA, IRFM
Saint-Paul-lez-Durance, France

Z. Lin
Department of Physics and Astronomy, University of California
Irvine, California, United States of America

JET Contributors*
*See the author list of "Overview of JET results for optimising ITER operation" by J. Mailloux *et al.* to be published in *Nuclear Fusion* Special issue: Overview and Summary Papers from the 28th Fusion Energy Conference (Nice, France, 10-15 May 2021)

Abstract

The interaction of Alfvén Eigenmodes (AEs) and energetic particles will determine the success of future tokamaks. In JET, eight in-vessel antennas were installed to actively excite *stable* AEs with frequencies ranging 25-250 kHz and toroidal mode numbers $|n| < 20$. During the 2019-2020 deuterium campaign, almost 7500 resonances and their frequencies, net damping rates, and toroidal mode numbers were measured in almost 800 plasma discharges. From a statistical analysis of the database, continuum and radiative damping are inferred to increase with edge safety factor, edge magnetic shear, and when including non-ideal effects. Both stable AE observations and their associated damping rates are found to decrease with $|n|$. The efficiency of active antenna excitation is also reduced in X-point vs limiter magnetic configuration and in H- vs L-mode. A novel measurement of marginal stability is reported for an edge-localized Ellipticity-induced AE (EAE) in the presence of fast ion populations resulting from ICRH and NBI heating powers up to 25 MW. NOVA-K kinetic-MHD simulations show good agreement with experimental measurements. Finally, *unstable* electromagnetic modes, with frequencies below Toroidicity-induced AEs (i.e. sub-TAE), are observed in JET plasmas with elevated q-profiles. These are postulated to be beta-induced ion temperature gradient (BTG) modes. Similar experimental and computational studies are planned for the recent hydrogen and ongoing tritium campaigns, in preparation for the DT campaign.

1. INTRODUCTION

The Alfvén Eigenmode Active Diagnostic (AEAD) actively excites stable Alfvén Eigenmodes (AEs) in JET tokamak plasmas. The importance of these AE stability measurements – i.e. frequencies $\omega_0 = 2\pi f_0$, net damping rates $\gamma < 0$, and toroidal mode numbers n – cannot be overstated. First, they provide a direct experimental comparison with net growth rates calculated from theory and simulation, from which the contributions of different driving and damping mechanisms can be assessed. Of particular interest is the measurement of alpha particle drive, which is a primary goal of energetic particle (EP) experiments and AEAD operation in the upcoming JET

DT campaign [1,2]. Importantly, the AEAD may be the only diagnostic capable of assessing this drive if the alpha population is insufficient to destabilize AEs. Finally, a better understanding of AE stability will improve projections of EP-driven AEs and the resulting AE-induced EP transport in next step tokamaks, such as ITER, and in future fusion pilot plants.

The JET AEAD comprises two in-vessel sets of four toroidally spaced antennas positioned below the midplane and on opposite sides of the torus [3]. Six amplifiers power six (of eight) antennas with currents ~6 A each; the resulting magnetic perturbation has magnitude $|\delta B/B| < 10^{-3}$ at the plasma edge. Independent phasing of the antennas allows power to be injected into a spectrum of toroidal mode numbers, $|n| < 20$ [4]. As the scanning antenna frequency passes through that of a stable AE, the plasma resonates like a driven, weakly damped harmonic oscillator [5], and the frequency-filtered magnetic response – obtained from a toroidal array of fast magnetic probes – determines f_0, γ, and n [6].

This paper reports on recent progress in experimental and computational studies of AE stability with the AEAD. In Section 2, an expanded database of AE and plasma parameters is presented, along with statistically significant trends related to AE physics. Section 3 focuses on the novel measurement of a stable AE during high external heating power, and experimental results are compared with kinetic simulations. In Section 4, low frequency modes in JET are identified and compared with gyrokinetic simulations. Finally, a summary is given in Section 5.

2. DATABASE STUDIES OF STABLE ALFVÉN EIGENMODES

This section presents a statistical analysis of thousands of stable AEs collected in the recent 2019-2020 JET D campaign (C38). The AEAD was operated on almost 800 plasma discharges, from which a database of almost 7500 stable AE measurements was assembled. Note that this database is actually an expansion of that reported earlier in [6] and [7] because new data were acquired after their publications.

In the following analyses, data are restricted to normalized damping rates $|\gamma/\omega_0| < 6\%$, uncertainties $|\Delta f_0| < 1$ kHz and $|\Delta\gamma/\omega_0| < 1\%$, X-point magnetic configuration, and heating powers from Neutral Beam Injection $P_{NBI} < 7$ MW and Ion Cyclotron Resonance Heating $P_{ICRH} < 7$ MW. The last two bounds are motivated by the sometimes-overwhelming pick-up in magnetics data which can lead to misidentification of AEs.

2.1. Trends in damping rate

Two recent works have analyzed stable AEs from the D campaign database: The damping rate was found to increase linearly with the edge safety factor q_{95} in [6]. This was attributed to an increase in continuum damping as the AE continuum gap closes at the plasma edge. The damping rate was also found to increase rapidly and nonlinearly with the edge magnetic shear s_{95} [7], likely due to both continuum and radiative damping. These trends are confirmed to have statistical significance in Table 1, which reports the linear correlation with γ/ω_0 weighted by its inverse variance (e.g. $|\Delta\gamma/\omega_0|^{-2}$). Here, magnitudes $|r_w| > 0.5$ are considered significant.

TABLE 1. WEIGHTED LINEAR CORRELATION WITH NORMALIZED DAMPING RATE

Parameter x	B_0	n_{e0}	T_{e0}	q_0	q_{95}	s_{95}	λ	P_{NBI}	P_{ICRH}
$r_w(\gamma/\omega_0, x)$	-0.16	-0.23	-0.02	-0.12	**0.53**	**0.57**	**0.70**	0.18	0.10

The highest correlation is with the so-called non-ideal parameter $\lambda = q_{95}s_{95}\sqrt{T_{e0}}/B_0$ [8,9], where T_{e0} and B_0 are the on-axis values of the electron temperature and toroidal magnetic field, respectively. Note that no correlation is observed with these quantities individually. The non-ideal parameter is key in the theory of radiative damping [9,10], and therefore λ is a better indicator of its impact than q_{95} or s_{95} alone. All data points are shown in Fig. 1a, where a clear linear trend is observed.

Correlations with NBI and ICRH powers are also given in Table 1. Here, data are restricted to non-zero input power since wide variation in the damping rate is observed with no external heating. With this filter, there are still

~400 and ~1000 data points for non-zero NBI and IRCH, respectively. While the correlations are relatively poor, linear fits to the damping rate do indicate increased damping with NBI and decreased damping with ICRH.

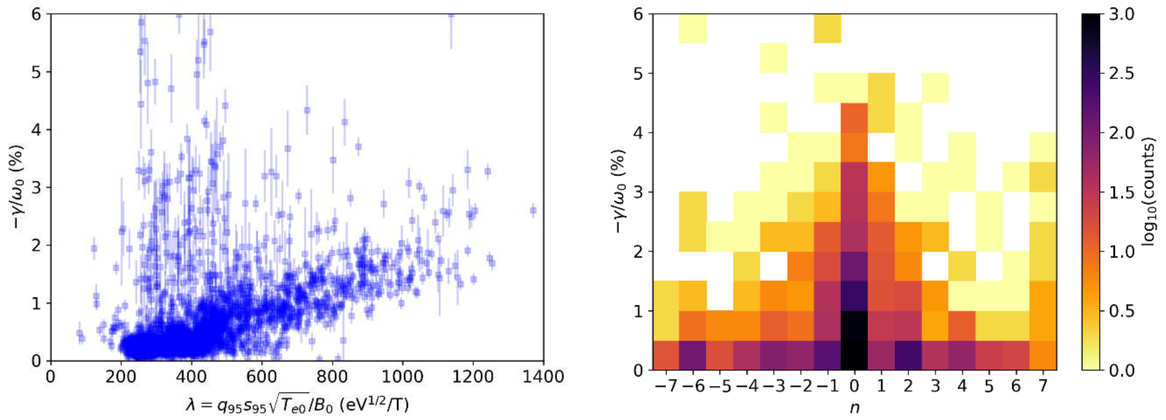

(a) (b)

FIG. 1. (a) Normalized damping rate vs non-ideal parameter, with uncertainties as error bars. (b) Number of stable AE observations (logarithmic) vs toroidal mode number ($|n|$ < 8) and normalized damping rate (uncertainties $|\Delta\gamma/\omega_0|$ < 0.5%).

2.2. Trends related to operational scenarios

Investigations of the AEAD operational space are also important, especially as they relate to high power, high performance scenarios and the upcoming JET DT campaign. In [6], it was reported that the AEAD's efficiency of resonantly exciting stable AEs decreased with increasing plasma current and external heating power. A thorough study of AEAD-plasma coupling [7] also showed reduced efficiency in X-point (i.e. diverted) magnetic configuration compared to limiter configuration – consistent with the q_{95} and s_{95} trends above – as well as with increased plasma-antenna separation.

More recently, an H-mode database [12] was compared with the stable AE database: Of the approximately 500 stable AEs measured in plasma discharges common to both databases, none were observed during H-mode periods. This confirms, with relatively high confidence (p-value = 0.076), that the AEAD cannot excite stable AEs during H-mode, likely due to the effect of the density pedestal on the AE continuum. Yet, there still exist some stable AE measurements during high power operation, as explored in Section 3.

Finally, the dependencies of the damping rate on toroidal mode number are explored. Figure 1b shows the number of stable AE measurements for each estimated n and bin of calculated γ/ω_0. Here, data are restricted to $|n|$ < 8, consistent with typical unstable AEs in JET, and uncertainty in the damping rate $|\Delta\gamma/\omega_0|$ < 0.5%, to better match the grid discretization. As discussed in [6], the high density of n = 0 values could indicate either true Global AEs (GAEs) or that too few magnetic probes were available for a good n estimation.

A general trend of decreasing $|\gamma/\omega_0|$ with $|n|$, also noted in [6], is observed in Fig. 1b. There are several possible explanations: For a given AE radial location, the mode width decreases as $1/|n|$ leading to more localized damping, as opposed to more global modes interacting with, say, the continuum. Also, in the presence of fast ions (FI), AE drive increases with n via $n\omega_{*FI} \propto \frac{n}{r}\frac{\mathrm{d}}{\mathrm{d}r}p_{FI}$, the FI pressure gradient. However, an asymmetry for positive and negative n would be expected, which is not easily observed. Unfortunately, even within a database of almost 7500 stable AEs, no $\pm n$ pair exists with sufficiently similar plasma (or FI) conditions to estimate $\mathrm{d}p_{FI}/\mathrm{d}r$ [13].

3. NOVEL MEASUREMENT OF AE STABILITY DURING HIGH POWER AUXILIARY HEATING

This section reports on a novel measurement of AE stability during high auxiliary heating, P_{NBI}+P_{ICRH} ~ 25 MW. This plasma (JPN 94703) was part of the three-ion-heating scenario development experiments at JET relevant to the upcoming JET DT campaign as well as ICRH in ITER [14,15]. Experimental results are presented in Section 3.1, and comparisons with kinetic simulations are given in Section 3.2.

3.1. Experiment

Time traces of plasma parameters for JPN 94703 are shown in Fig. 2a, with the time range of interest, t = 8-12 s, shaded. Flattop parameters are B_0 = 3.7 T, I_P = 2.5 MA, n_{e0} ~ 8e19 m^{-3}, and T_{e0} ~ 5 keV. Auxiliary heating are P_{NBI} ~ 19-21 MW and P_{ICRH} ~ 4.4 MW from t = 8-11 s. Plasma profiles are shown for one time, t = 8.5 s, in Fig. 2b. The q-profile is from EFIT constrained by the fitted kinetic profiles from TRANSP [16,17], which match Thomson Scattering n_e and T_e data well. (Here, equal electron and ion temperatures, T_e = T_i, are assumed.) Rotation data is obtained from ^{3}He charge exchange spectroscopy. Note that while there is a density pedestal, there is none for electron temperature; thus, this plasma is in L-mode, and the AEAD can excite stable AEs.

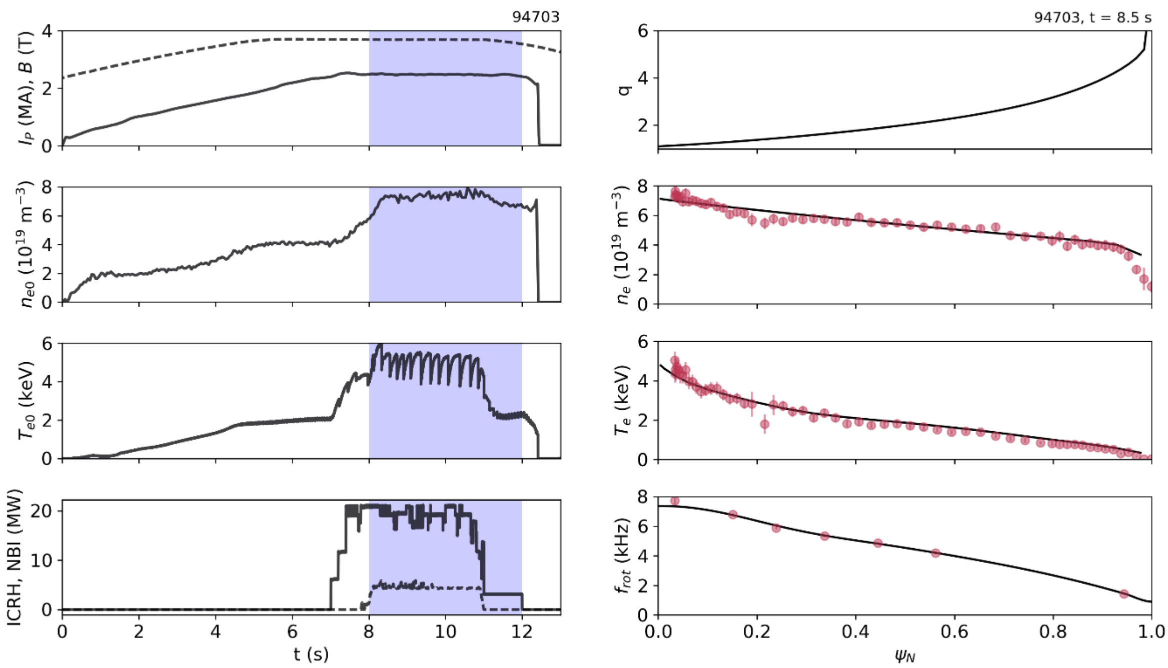

(a) (b)

FIG. 2. (a) Plasma parameters for JPN 94703: toroidal magnetic field (dashed), plasma current (solid), central electron density and temperature from Thomson Scattering (TS) and Electron Cyclotron Emission, respectively, and heating powers from NBI (solid) and ICRH (dashed). A stable AE was tracked during the shaded time interval. (b) Profiles at t = 8.5 s: safety factor from a pressure-constrained EFIT, electron density and temperature from TS, and rotation frequency from ^{3}He charge exchange. Experimental data are shown as circles with uncertainties as error bars, while solid lines are fitted data.

A stable AE was tracked in real time during the high heating power phase. This can be seen in the spectrogram of Fig. 3a. The triangular waveform is the scanning AEAD frequency, f = 125-250 kHz. The antenna phasing was such that power was injected primarily into odd toroidal mode numbers (i.e. $|n|$ = 1, 3, 5,…) which is confirmed by the mode number analysis of the magnetic probes, showing primarily n = 3 (magenta). Around t = 8.5 s, a stable AE is detected at f_0 ~ 235 kHz, but is then quickly lost by the real-time tracking system. A marginally unstable AE is seen between t ~ 9-10 s with a mix of n = 0 (grey) and n = 5 (cyan). The AEAD finds the stable mode again at t ~ 10.5 s and then tracks until t ~ 12 s when f_0 ~ 250 kHz.

The measured stable AE parameters are shown in Fig. 3b. Here, the same AE resonance must be detected by at least 3 (of 14) magnetic probes to be considered "good." Characteristic peaks in the magnetic response (summed from all probe amplitudes) are observed, though they are easier to identify by eye later in time. The resonant frequency of the AE is relatively smooth in time, and so is the damping rate -γ/ω_0 ~ 0.25% (-γ ~ 0.6 kHz), indicating marginal stability. Note how γ/ω_0 does not change as NBI power is reduced from t ~ 10.5-11 s.

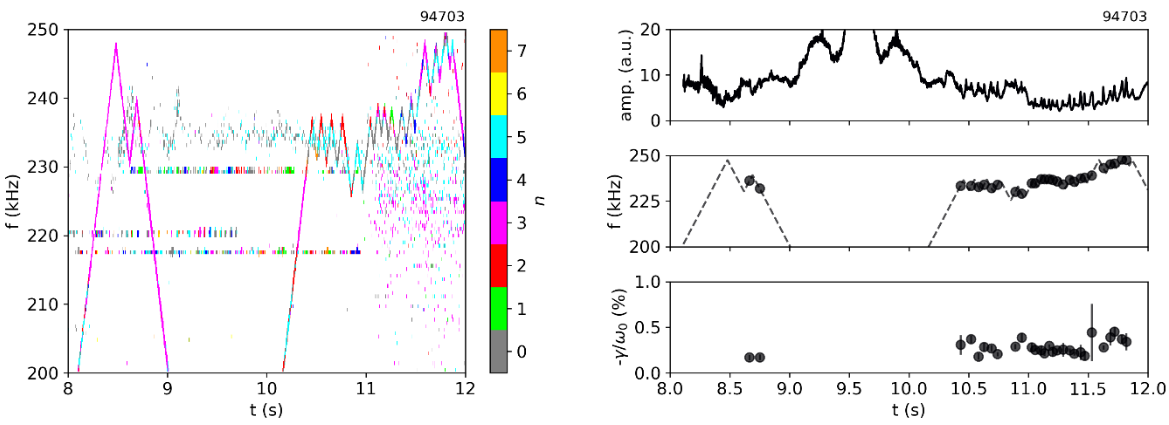

(a) (b)

FIG. 3. (a) Spectrogram with toroidal mode number analysis. (b) Stable AE resonance measurements: the magnetic response amplitude (summed over all probes), AEAD (dashed) and resonant frequencies (circles), and normalized damping rates with uncertainties as error bars.

3.2. Simulation

While the mode number identification of n = 5 seems clear in Fig. 3a, this result is unfortunately quite sensitive to the magnetic probes used. In fact, a separate analysis of the resonances (not shown) returns a range $|n|$ = 0-5. Additionally, the stable AE's location is difficult to identify because the antenna perturbation is small and is thus not seen in the Fourier analysis of interferometry, reflectometry, or soft X-ray data. That said, the AEAD is known to excite more edge-localized AEs as an external antenna [6]. Thus, a range of mode numbers $|n|$ = 3-6 is simulated with the NOVA-K kinetic-MHD code [18-20] to assess the existence, mode structure, and stability of AEs. Input profiles are those at t = 8.5 s (Fig. 2b), approximately the time of the first stable AE measurement (Fig. 3b).

NOVA-K also calculates the contribution to the growth rate from NBI ions, assuming a slowing down distribution.[1] In JPN 94703, D-NBI ions, with energies ~100 keV, were injected with normal and tangential beams with initial pitches $v_{\parallel}/v_0$ ~ 0.44 and 0.62, respectively. The D fast ion distribution function is computed in TRANSP using the NUBEAM and TORIC modules, with NBI and IRCH synergy accounted through the Monte Carlo kick model. The pitch- and flux-surface-averaged fast ion distribution is shown in Fig. 4a. The bulk NBI population is clearly seen below ~0.1 MeV with broad radial extent. The fast ion tail, accelerated by ICRH, extends to ~2.5 MeV and is core-localized, yet is insufficient to destabilize AEs in this plasma.

NOVA-K simulations identify three candidate AEs – i.e. EAEs in the edge gap – with similar frequencies and net damping rates as the experimentally measured mode. Their toroidal mode numbers, resonant frequencies, and breakdown of damping rate contributions are provided in Table 2. Note that the 23% ^{3}He has not been simulated here,[1] but its expected effect is to only increase the Alfvén speed (and hence the plasma-frame AE frequency) by ~6%, which is approximately the same uncertainty introduced by any fitted profile.

The simulated n = 5 mode, with lab-frame frequency f_0 ~ 236 kHz and net damping rate -γ/ω_0 ~ 0.34%, is the best match with the experimental AE. The poloidal mode structure is plotted with the Alfvén continuum in Fig. 4b, with dominant couplings of poloidal harmonics m = (9,11), (10,12), and (11,13). Its localization around $\sqrt{\psi_N}$ ~ 0.7-0.9 (ψ_N ~ 0.5-0.8) is consistent with improved AEAD coupling to the edge as opposed to core modes.

From Table 2, the dominant contributions to the AE's marginal stability are electron Landau and continuum damping, with small contributions from NBI fast ion and electron collisional damping. The almost negligible damping from NBI fast ions < 100 keV makes sense since their parallel injection velocities are less than both the

[1] The contributions from ICRH-accelerated fast ions and non-negligible minority species are currently being incorporated into NOVA-K and thus were not considered in the present work.

Alfvén speed v_A ~ 7e6 m/s and side-band resonance $v_A/3$. Both radiative and ion Landau damping are negligible here. The damping mechanisms of this edge-localized EAE are very different from that of the core-localized TAE in JET studied earlier [21], which is expected given the different AEs, localizations, and plasma scenarios.

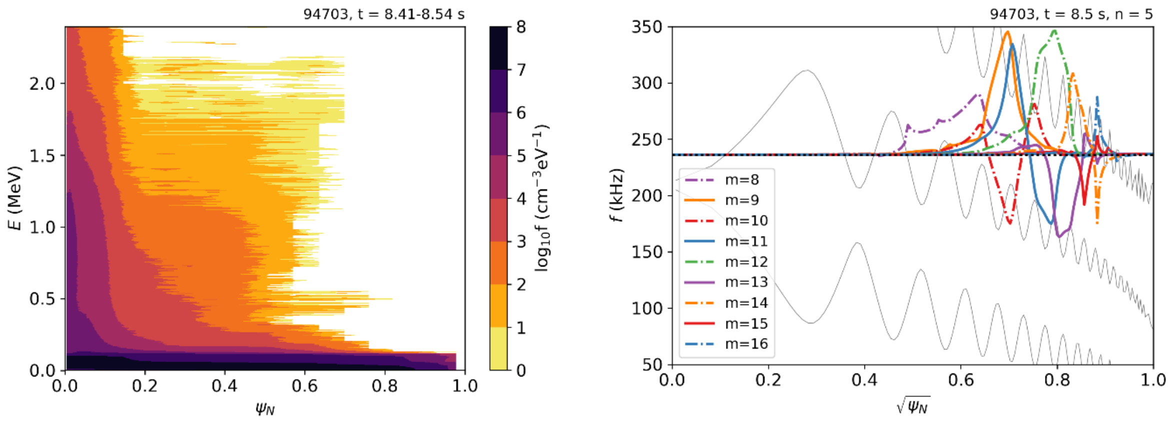

(a) (b)

FIG. 4. (a) Pitch- and flux-surface-averaged D fast ion distribution function (logarithmic) from TRANSP for JPN 94703 and integrated over t = 8.41-8.54 s. (b) Continua (thin lines) and poloidal mode structure (solid, dot-dashed) from NOVA-K at t = 8.5 s for n = 5. The frequency (lab-frame) is indicated by the horizontal dotted line. ψ_N is the normalized poloidal flux.

TABLE 2. NORMALIZED DAMPING RATE (%) CALCULATED FROM NOVA-K

Damping γ/ω_0 (%)	n = 3, f_0 = 243.1 kHz	n = 5, f_0 = 236.4 kHz	n = 6, f_0 = 232.7 kHz
Continuum	-0.092	-0.116	-0.177
Radiative	0.000	0.000	0.000
Electron collisional	-0.011	-0.010	-0.010
Electron Landau	-0.161	-0.198	-0.176
Ion Landau	~0.000	~0.000	~0.000
NBI fast ions	-0.031	-0.017	-0.014
Total	**-0.295**	**-0.341**	**-0.378**

4. IDENTIFICATION OF ELECTROMAGNETIC MODES IN THE SUB-TAE FREQUENCY RANGE

Electromagnetic (EM) modes are often observed in the sub-TAE frequency range in JET plasmas with elevated q-profiles; these have recently been identified as beta-induced ion temperature gradient (BTG) driven eigenmodes [22]. They are characterized in experiment by the following requirements: (i) a high ion beta regime with a significant thermal ion temperature gradient (often related to an Internal Transport Barrier), (ii) a localization near a rational magnetic surface with a low magnetic shear, (iii) a strong thermal ion dependence, scaling with the ion drift frequency, and (iv) a coupling among Alfvén, acoustic, and drift waves. In [22], these characteristics are also compared with the analytical theory of BTG modes [23] as well as linear gyrokinetic simulations with the Gyrokinetic Toroidal Code (GTC) [24] using a realistic magnetic geometry and plasma profiles.

A good example of BTG modes is JPN 95649, a recent pulse during D experiments dedicated to scenario development for the study of energetic particles and EP modes in DT [1,2]. Figure 5a shows time traces of plasma parameters, with the time range of interest, t = 6.5-6.9 s, shaded. Plasma parameters during this phase are B_0 = 3.3 T, I_P ~ 2.7 MA, n_{e0} ~ 1e20 m^{-3} and T_{e0} ~ 7 keV (not shown), while auxiliary heating powers are P_{NBI} ~ 15-22 MW and P_{ICRH} ~ 2 MW. Also shown in Fig. 5a is the time trace of the neutron rate; a "roll-over" is observed around t ~ 6.7 s, which is currently being investigated in its relation to the BTG modes. These are seen in Fig. 5b as broadband, low (sub-TAE) frequency modes (f ~ 20-140 kHz in the lab frame) with toroidal mode numbers n = 1-7.

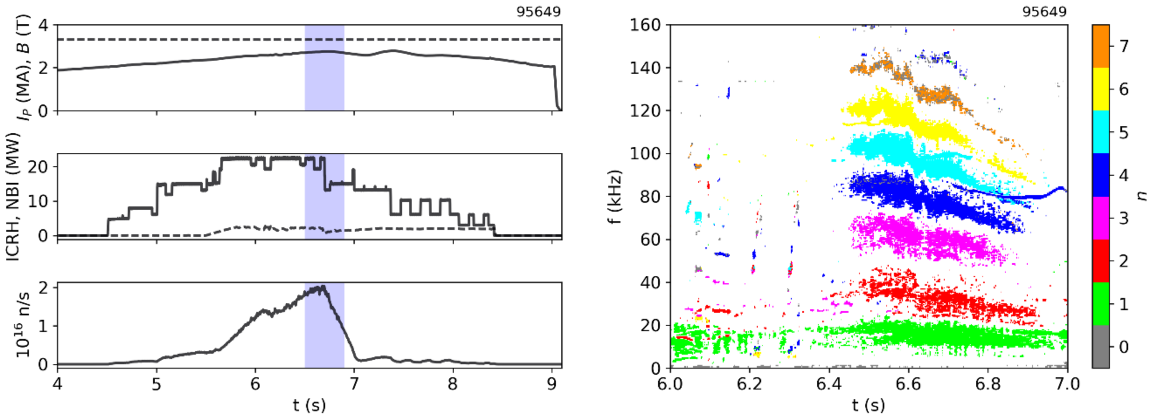

(a) (b)

FIG. 5. (a) Plasma parameters for JPN 95649: toroidal magnetic field (dashed), plasma current (solid), heating powers from NBI (solid) and ICRH (dashed), and neutron rate. Unstable sub-TAE modes were observed during the shaded time interval. (b) Spectrogram with toroidal mode number analysis.

5. SUMMARY

Understanding the interaction of Alfvén Eigenmodes (AEs) and energetic particles (EPs) is important to the success of future tokamaks. In JET, eight toroidally spaced, in-vessel antennas – collectively called the Alfvén Eigenmode Active Diagnostic (AEAD) – actively excite *stable* AEs with frequencies ranging f = 25-250 kHz and toroidal mode numbers $|n|$ < 20. The AEAD is an important diagnostic when AEs are not destabilized by EPs, which could even be the case for alpha drive in the upcoming JET DT campaign.

During the 2019-2020 deuterium campaign, ~7500 resonances – along with their frequencies $\omega_0 = 2\pi f_0$, net damping rates $\gamma < 0$, and toroidal mode numbers n – were measured in ~800 plasma discharges. A statistical analysis was performed on the database: continuum and radiative damping were found to increase with edge safety factor, edge magnetic shear, and when including non-ideal effects (see Table 1 and Fig. 1a). The number of stable AEs and their corresponding damping rates were found to decrease with $|n|$ (see Fig. 1b). Finally, the AEAD was found to be less efficient in exciting stable AEs (i) in X-point versus limiter magnetic configuration and (ii) in H- versus L-mode.

A novel measurement of marginal AE stability was presented for a plasma with a fast ion population resulting from ICRH and NBI heating powers up to 25 MW (see Figs. 2 and 4a). A stable AE was tracked in real time with frequency f_0 ~ 235-250 kHz, net damping rate γ/ω ~ -0.25%, and estimated toroidal mode number $|n|$ ~ 3-6 (see Fig. 3). NOVA-K kinetic-MHD simulations showed good agreement with experimental measurements, indicating the dominance of electron Landau and continuum damping for a marginally stable, edge-localized EAE (see Table 2 and Fig. 4b).

Lastly, low frequency (sub-TAE) electromagnetic modes were observed in JET plasmas with elevated q-profiles (see Fig. 5). Postulated to be beta-induced ion temperature gradient (BTG) modes, these were found to be consistent with both analytic theory and linear gyrokinetic GTC simulations in [22]. Similar experimental and computational studies are planned for the 2020 hydrogen and 2021 tritium campaigns, in preparation for the upcoming JET DT campaign.

ACKNOWLEDGEMENTS

The authors thank Y. Kazakov, M. Nocente, J. Ongena, M. Baruzzo, P. Bonofiglo, N. Dreval, L. Frassinetti, N. Gorelenkov, V. Guillemot, N. Hawkes, S. Menmuir, F. Nave, M. Podesta, E. Rachlew, Ž. Štancar, G. Szepesi, and A. Teplukhina. This work was supported by US DOE DE-FG02-99ER54563, DE-AC05-00OR22725, and DE-AC02-05CH11231. This work has been carried out within the framework of the EUROfusion Consortium and has received funding from the Euratom research and training program 2014-2018 and 2019-2020 under grant agreement No 633053. The views and opinions expressed herein do not necessarily reflect those of the European Commission.

REFERENCES

[1] DUMONT, R.J., MAILLOUX, J., ASLANYAN, *et al.*, Scenario development for the observation of alpha-driven instabilities in JET DT plasmas, Nucl. Fusion **58** 8 (2018) 082005.

[2] JOFFRIN, E., ABDUALLEV, S., ABHANGI, M., *et al.*, Overview of the JET preparation for deuterium-tritium operation with the ITER like-wall, Nucl. Fusion **59** 11 (2019) 112021.

[3] PANIS, T., TESTA, D., FASOLI, A., *et al.*, Optimization of the active MHD spectroscopy system on JET for the excitation of individual intermediate and high-n Alfvén eigenmodes, Nucl. Fusion **50** 8 (2010) 084019.

[4] PUGLIA, P., PIRES DE SA, W., BLANCHARD, P., *et al.*, The upgraded JET toroidal Alfvén eigenmode diagnostic system, Nucl. Fusion **56** 11 (2016) 112020.

[5] FASOLI, A., BORBA, D., BOSIA, G., *et al.*, Direct measurement of the damping of toroidicity-induced Alfvén Eigenmodes, Phys. Rev. Lett. **75** 645 (1995).

[6] TINGUELY, R.A., PUGLIA, P.G., FIL, N., *et al.*, Results from the Alfvén Eigenmode Active Diagnostic during the 2019-2020 JET deuterium campaign, Plasma Phys. Control. Fusion **62** 11 (2020) 115002.

[7] TINGUELY, R.A., PUGLIA, P.G., FIL, N., *et al.*, Experimental studies of plasma-antenna coupling with the JET Alfvén Eigenmode Active Diagnostic, Nucl. Fusion **61** 2 (2021) 026003.

[8] HEIDBRINK, W.W., FASOLI, A., BORBA, D., JAUN, A., Stable ellipticity-induced Alfvén eigenmodes in the Joint European Torus, Phys. Plasmas **4** 3663 (1997).

[9] PANIS, T., FASOLI, A., TESTA, D., *et al.*, Analysis of damping rate measurements of toroidal Alfven eigenmodes on JET as a function of n: part I. Nucl. Fusion **52** 3 (2012) 023013.

[10] METT, R.R., MAHAJAN, S.M., Kinetic theory of toroidicity-induced Alfvén eigenmodes, Phys. Fluids B: Plasma Physics **4** 2885 (1992).

[11] METT, R.R., STRAIT, E., MAHAJAN, S.M, Damping of toroidal Alfvén modes in DIII-D, Phys. Plasmas **1** 3277 (1994).

[12] FRASSINETTI, L., SAARELMA, S., VERDOLAEGE, *et al.*, E., Pedestal structure, stability and scalings in JET-ILW: the EUROfusion JET-ILW pedestal database, Nucl. Fusion **61** 1 (2021) 016001.

[13] FASOLI, A., TESTA, D., SHARAPOV, S., *et al.*, MHD spectroscopy, Plasma Phys. Control. Fusion **44** 12B (2002) B159.

[14] KAZAKOV, Y., NOCENTE, M., MANTSINEN, M.J., et al., Plasma heating and generation of energetic D ions with the 3-ion ICRF + NBI scenario in mixed H-D plasmas at JET-ILW, Nucl. Fusion **60** 11 (2020) 112013.

[15] NOCENTE, M., KAZAKOV, Y., GARCIA, J., *et al.*, Generation and observation of fast deuterium ions and fusion-born alpha particles in JET D-^{3}He plasmas with the 3-ion radio-frequency heating scenario, Nucl. Fusion 60 **12** (2020) 124006.

[16] HAWRYLUK, R.J., An empirical approach to tokamak transport, Phys. of Plasmas Close to Thermon. Cond. **1** 19 (1980).

[17] ONGENA, J.P.H.E., VOITSEKHOVITCH, I., EVRARD, M., MCCUNE, D., Numerical Transport Codes, Fusion Sci. Technol. **61** 2T (2012) 180–189.

[18] CHENG, C.Z., Kinetic extensions of magnetohydrodynamics for axisymmetric toroidal plasmas, Phys. Rep. **211** 1 (1992).

[19] FU, G.Y., CHENG, C.Z., Excitation of high-n toroidicity-induced shear Alfvén eigenmodes by energetic particles and fusion alpha particles in tokamaks, Phys. Fluids B: Plasma Physics **4** 3722 (1992).

[20] GORELENKOV, N.N., CHENG, C.Z., FU, G.Y., Fast particle finite orbit width and Larmor radius effects on low-n toroidicity induced Alfvén eigenmode excitation, Phys. Plasmas **6** 2802 (1999).

[21] ASLANYAN, V., TAIMOURZADEH, S., SHI, L., *et al.*, Gyrokinetic simulations of toroidal Alfvén eigenmodes excited by energetic ions and external antennas on the Joint European Torus, Nucl. Fusion **59** 2 (2019) 026008.

[22] FIL, N., SHARAPOV, S., FITZGERALD, M., *et al.*, and JET CONTRIBUTORS, Interpretation of electromagnetic modes in the sub-TAE frequency range in JET plasmas with elevated q-profile, (in preparation).

[23] MIKHAILOVSKII, A.B., SHARAPOV, S.E., Beta-induced temperature-gradient eigenmodes in tokamaks, Plasma Phys. Rep. **25** (1999).

[24] LIN, Z., HAHM, T.S., LEE, W.W., TANG, W.M., WHITE, R.B., Turbulent transport reduction by zonal flows: massively parallel simulations, Science **281** 5384 (1998) 1835–1837.